Int. J. Electrochem. Sci., 14 **(2019)** 3949 – 3967, doi: 10.20964/2019.04.02

International Journal of
ELECTROCHEMICAL
SCIENCE
www.electrochemsci.org

Review

Mechanistic Aspects of Factors Affecting Pitting Corrosion of Metallic Materials for Marine Application: A Review Paper

Shicheng Wei[*], *Hongyi Su*

National Key Laboratory for Remanufacturing, Army Academy of Armored Forces, Beijing 100072, China
[*]E-mail: wsc33333@163.com

Received: 24 October 2018 / *Accepted:* 24 December 2018 / *Published:* 10 March 2019

Seawater as an electrolyte makes metals and alloys suffer from corrosion deterioration. Among various corrosion forms, pitting corrosion is extremely hazardous for marine structures. It degrades the performance of metal materials and reduces the service life of equipment and facilities. The theory concerning pitting corrosion has gained a certain process. However, its behavior and mechanism in some special environments such as deep-sea environment are still not fully understood. Hence, a review involving these issues is a need. This paper summarizes the current progress in aspects of pit mechanism including pit initiation, metastable pit, propagation of pit and its affecting factors. The focus is the influencing mechanism of three interesting factors on metal corrosion covering passive film, hydrostatic pressure and mechanical load.

Keywords: Pitting corrosion; Passive film; Hydrostatic pressure; Mechanical load

1. INTRODUCTION

The scientific activities and exploitation of mysterious ocean are proceeding at a high rate, bringing the rapid development of metallic materials for marine application. They are used in the construction offshore platforms, ships, underwater robot, deep-sea submersible, etc. due to good mechanical properties. However, most of them are susceptible to pitting corrosion in aggressive marine environment [1]. As one of the most hazardous forms of corrosion, it is usually the initiation of stress corrosion and corrosion fatigue crack, leading to the early catastrophic failure of structural materials. [2,3]. Consequently, extensive concern toward their reliability has been given by many scientific researchers.

Pitting corrosion phenomena have been investigated for several decades. Some related theories have been reviewed by Kolotyrkin [4], Szklarska-Sialowska [5,6] and Frankel [7]. They have

summarized some basic conclusions. However, it can be known in their reviews that a deeper insight into pitting corrosion process in atomic scale is still in need. Recently, Soltis [8] has given a detailed overview of pitting theory about metallic materials, focusing on events associated with passivity breakdown, pit initiation and pit growth. Meanwhile, Bhandari et al. [9] provide a technical review concerning pitting corrosion behavior of steels in marine environment and some typical affecting factors. However, mechanistic opinions are limited in their reports and several critical factors are not covered. In recent years, more and more corrosion researchers put their attention into passive film, hydrostatic pressure and mechanic load that have a significant impact on the corrosion behavior of metals and alloys. This part of the work has achieved considerable progress and needs to be reviewed timely for a favor of theoretical research and optimization of materials.

2. CHARACTERISTICS OF PITTING CORROSION

Pitting corrosion is defined as a localized accelerated dissolution of metal such as stainless steels, Fe-Cr alloy, Al alloy and nickel. Its initiation is usually related with the flaw or a breakdown in passive film covered on the metal surface [7,10]. Events associated with pits occur randomly in space and time on metal surface that is exposed to aggressive solution and initiate at a nanometer scale. Moreover, its propagation process is autocatalytic in nature and hard to detect.

Pitting potential, E_{pit} [11], and repassivation potential, E_r [12], are two typical parameters used to depict pitting corrosion. For E_{pit}, it is defined as the lowest potential that can maintain the stable propagation of pit and characterized by a sudden increase of current density in the anodic polarization curves [13-15]. More noble potential for E_{pit} means that it takes shorter time for pitting initiation. E_r is described as the potential that above which metastable pits have capacity to form and the existing pits can propagate again. It becomes a drop in current of cyclic voltammetry curves [16]. Both parameters are associated with testing parameters and environmental factors such as scan rate of electrochemical testing system [17,18], chloride concentration [19], pH [20], magnetic field [21], flow velocity [22], hydrostatic [23] the nature of metallic material and some other factors [24,25]. In general, E_{pit} preferentially increases with the increase of potential scan rate, but it shows independence of scan rate for Al or Al5Zn alloy. Additionally, E_{pit} is a function of the chloride concentration and its activity. As the inhibiting ions remain constant in electrolyte, E_{pit} decreases as the chloride concentration increases, showing a semi-logarithmic relationship. In general, the higher the chloride activity, the lower the E_{pit} is. The accelerated pitting corrosion phenomena for many metals at high temperature or hydrostatic pressure is usually caused by the increased chloride activity. It can decrease E_{pit} due to the improvement of the interaction between chloride and metal surface.

2.1 Passivity breakdown

The process of pitting growth has been identified as distinct steps, namely passivity breakdown, pit initiation, metastable propagation and stable propagation. It is generally accepted that the passivity

loss of passive metal and the origin of corrosion pits can be mainly caused by three mechanisms: penetration mechanism, film breakdown mechanism and adsorption mechanism [7]. In penetration mechanism, the aggressive ions with small size such as Cl^-, Br^- and I^- have a ability to penetrate the oxide film under the condition of high electric field and incorporate into the film, forming a penetration path that is more electrically conductive than the origin one [26-30]. The reaction between penetrated ions with oxide lattice leads to the vacancy at the metal-film interface, so that the film possibly undergoes destruction by local stress caused by the condensation of vacancy [31-33].

Compared with penetration mechanism, the model in film breakdown mechanism considers that the appearance of breaks in passive film is caused by the adsorption of aggressive ions rather than the local stress at the metal-film interface. These adsorbed ions can reduce the surface tension of passive film, inducing its crack and providing a path for the diffusion of anions [34-36]. The pressure vertically applied on the film is related with the decreased surface tension, film thickness and electric fields across the film [36]. As it exceeds to a critical breakdown stress, the crack will arise in passive film, causing pit initiation.

The adsorption mechanism involves the adsorption of aggressive anions on the surface of oxide film, leading to the hybridization of oxide lattice in the surface layer. The anions can more easily transfer from electrolyte to oxide film [37-39]. Hence, oxide films preferentially dissolute at the sites where aggressive ions are adsorbed. Due to higher electrical field strength across the oxide film, the migration of metal ions can be accelerated. The increased local dissolution at these sites encourages the initiation of pits [40-42].

Other mechanisms are associated with the chemical composition difference on metal surface that is the onset of pitting initiation. Sites of chemical composition difference include the irregular arrangement of Fe and Cr in binary lattice [43-47], inclusion (usually MnS, CaS, $MnAl_2O_4$ or Al_2O_3) [48-51] and metal-inclusion interfaces [52-56]. The galvanic couple formed by connecting the area of composition segregation with matrix induces the initiation of pits. In recent years, the observations of pitting initiation at the metal-inclusion interface were well characterized on a nanometer scale by many researchers. Some chromium-depleted zones around MnS particle illustrated in Fig. 1 were found by Ryan et al. [57] An iron sulphide enriched ‘halo’ near MnS inclusion with a thickness up to 100nm was detected by Williams et al. [58] Additionally, Jin et al. [59] examined the electrochemical heterogeneity between inclusion and the adjacent steel matrix by localized electrochemical impedance spectroscopy.

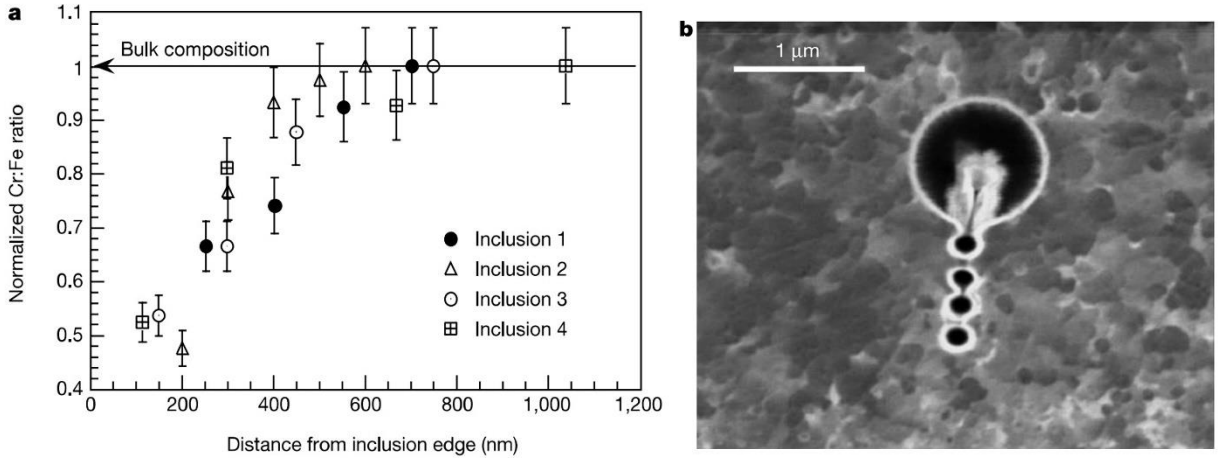

Figure 1. Local FIB-SIM analysis adjacent to MnS particles in 316 stainless. (a) Normalized Cr/Fe ratio as a function of proximity to a sulphide inclusion. (b) Secondary electron images of the surface after SIMS analysis. Reprinted with permission from reference 57. Copyright 2018 Springer Nature.

2.2 Metastable pitting

Metastable pitting, a critical stage of pitting corrosion, occurs below the critical pitting potential. There is an induction time before the onset of stable pits [60,61]. The transition from metastable growth to stable growth depends on a certain condition and the dynamic aspects concerning this transition is a need for further research [62-64]. It has been widely observed that some fluctuations of current exist before the formation of stable pits. Different stages of corrosion pits before stable pits can be distinguished from the tendency of current [65-69]. The current that rises suddenly, decays continuously and slowly decreases to background level presents the nucleation of pits [70,71[, while the current that rises slowly, followed by sudden decay demonstrates the metastable growth of pits, as shown in Fig. 2 [72,73].

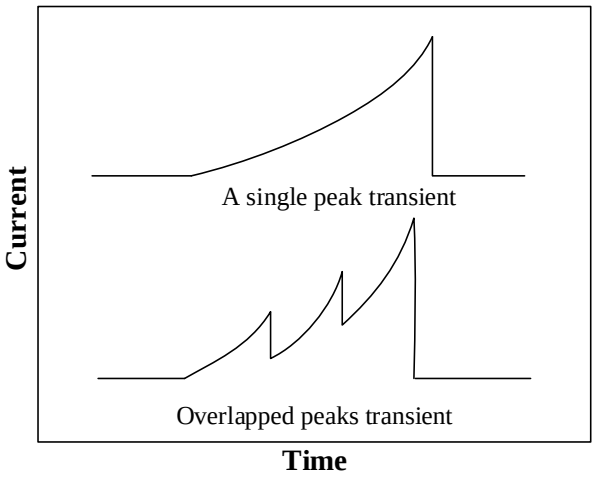

Figure 2. Current transients of the growth of metastable pit on stainless steel.

The dynamic of metastable growth is related to the potential, local chloride concentration and pH reduction inside the pit. The passivity of metals is possibly interrupted even below the critical pitting potential due to the existence of aggressive anions [74]. Under a certain condition, metastable pits can continuously propagate at a potential lower than pitting potential and this condition is determined by the active dissolution of metal and the diffusion of metal cations from the pit to the bulk solution [75-78]. As the diffusion rate of metal cations is lower than the dissolution rate of metal, the hydrolysis of dissolved metal cations will give rise to local acidification inside the pit accompanied by increased chloride concentration and pH reduction. As a result, the propagation of metastable pits can be further accelerated [79-81].

2.3 Pit propagation

As a pit propagates, the metal will dissolute at a high rate within the occluded cavity while the adjacent areas around pits sustain passive state. This process is predominated by the diffusion of ions [82-86]. The growth dynamics of pits relate with the local acidic conditions in the interior of pits. This opinion was first proposed by Hoar [87]. Afterwards, Galvele [88] developed a detailed model to describe the pitting propagation caused by localized acidification. In this model, it is assumed that there is always a passive film existing on the metal surface and the metastable pit is the evidence for film rupture and its self-healing process. Galvele found that localized acidification depends on pit depth, x, and current density, i. It is a function of $x \bullet i$ that is a critical parameter to determine whether the pit is in propagation or repassivation. The propagation of pits is an autocatalytic process [89-92]. Metal on surface dissolves due to the attraction of aggressive ions such as Cl^-. The hydrolysis of metal ions leads to the reduction of pH and the reaction is given by:

$$Me + n\,Cl \rightarrow MeCl_n \quad (1)$$

$$Me^{n+} + H_2O \rightarrow Me(OH)^{(n-1)+} + H^+ \quad (2)$$

To balance the electron equilibrium within the cavity, the Cl^- from the bulk electrolyte transfers into the cavity, resulting in the increase of chloride concentration, therefore, further stimulating the growth of pits [90-92].

3. FACTORS AFFECTING PITTING CORROSION

Seawater is an electrolyte enriched in aggressive Cl^- where metallic materials usually subject to pitting corrosion. The influencing factors in filed environment associated with metal corrosion involves temperature, dissolved oxygen, pH, salinity, protective film, flow velocity, hydrostatic pressure, mechanical load, metallurgical factors, etc. The aspects about the relationship between a part of typical factors with pitting corrosion has accessed considerable achievements and this part of content has been reviewed by Frankel [7], Soltis [8], and Bhandari et al. [9]. They mainly consist of temperature, dissolved oxygen, pH and salinity. Due to the increasing interest in the ocean depth and field operating condition, the factors of passive film, hydrostatic pressure and mechanical load gain more and more interest of

scientists and engineers in the past decades, which is presented in the following sections.

3.1 Passive film

It is well known that passive film can provide an excellent protection to the uniform corrosion attack for passivated metals and alloys due to their dense structure and good adhesion to steel surface However, these films are susceptible to local dissolution or breakdown, leading to the initiation of pits. As a result, it is beneficial to give an insight into the nature of passive film, its growth mechanism and breakdown.

3.1.1 The nature of passive film

Generally, the passive film on stainless steel [93-98], Fe-Cr alloy [99-104] and Fe-Cr-Ni alloy [105-109] exhibits a distinct bi-layer structure with a Cr-oxide inner layer and Fe-oxide outer layer, which possess a few nanometers in thickness.

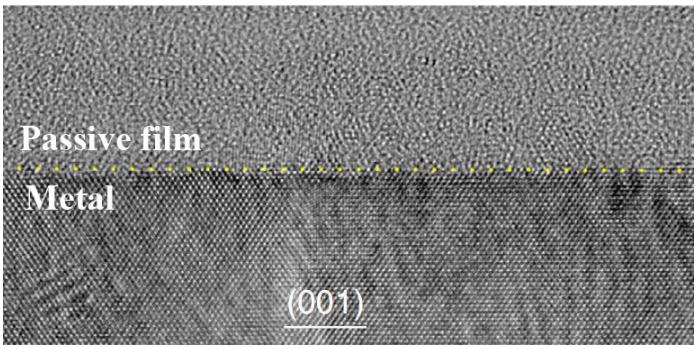

Figure 3. HRTEM images of Fe-Cr-Ni alloy on which a passive film has been formed in 0.5 mol L^{-1} H_2SO_4 electrolyte. Reprinted with permission from reference [109]. Copyright 2018 Springer Nature.

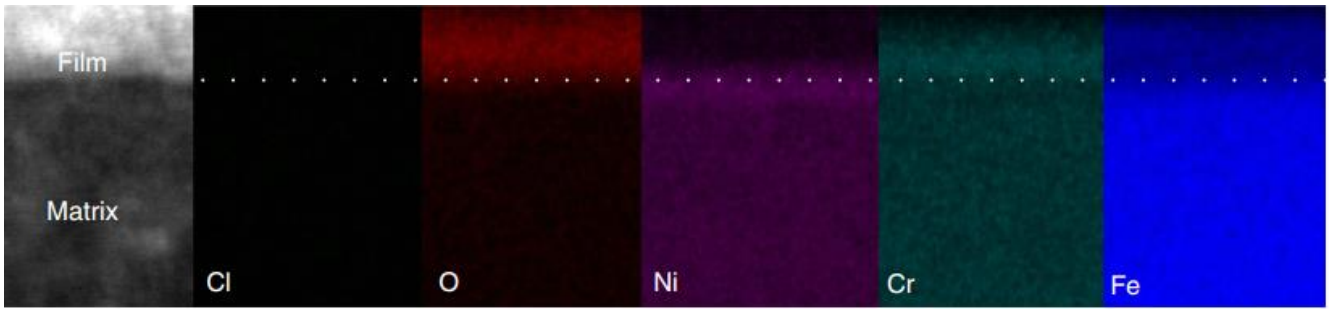

Figure 4. EDS line profile at the cross section of passive film on stainless steel by aberration corrected HRTEM. Reprinted with permission from reference [109]. Copyright 2018 Springer Nature.

Fig. 3 presents a cross-sectional HRTEM images of the passive film formed on Fe-Cr-Ni alloy [109]. The passive film with a thickness of several nm shows an amorphous structure, in which some nanocrystals are embedded. The information of element distribution at a cross section of Fe-Cr-Ni alloys

is illustrated in Fig. 4. The Cr enriched site locates in the lower part of the passive film with a depletion and an enrichment of Fe distributes in the upper part of the passive film, which demonstrates their bi-layer structure. Mott-Schottky plots also well describe the duplex layer of passive films that have an p-type inner chromium oxide layer and an n-type outer iron oxide layer [110-113].

3.1.2 The growth of passive film

The nucleation and growth of passive film on the metal surface depend on the solution environment and applied potentials. In alkaline aqueous solution, the onset of the growth of passive film is the adsorption of OH^- at low potential, followed by the reaction [114-116]:

$$Me + nOH^- \rightarrow Me(OH)_n + ne^- \quad (3)$$

Therefore, it induces the formation of a 2D adlayer which is a precursor for the growth of 3D oxide film. For a single-crystal passivated metal with smooth terraces on its surface, the nucleation generally occurs at the step edges, which possesses higher reactivity due to more pre-existing defects. Metal at these sites preferentially reacts with OH^-, forming poorly crystallized hydroxide. The reactive regions expand laterally with time and finally cover completely the terraces. 3D growth of oxide film on the preformed 2D adlayer is predominated by applied potentials corresponding to the driving force for oxide formation. As the potential exceeds a critical value, the 2D adlayer grows along the direction perpendicular to the metal surface and forms well crystallized oxide film with a thickness of several monolayer [115-117]. As for stainless steels with polycrystalline structure, the thickness of passive film can grow from several nanometers to dozens of nanometers with increasing potential. Crystalline structure and amorphous phase can be at the same time obtained at various potentials [118-124].

The growth of passive film, a thermodynamic dynamically process, can be interpreted by the chromium passivation mechanism in acidic solution. As the metal with a fresh surface is exposed to acidic media, the active chromium is covered by a hydride layer preceding the formation of passive state [125-127]. The reaction is given by:

$$2CrH + 2H_2O \rightarrow Cr_2O_3 + 8H^+ + 8e^- \quad (4)$$

Because of much lower potential for the stable growth of Cr_2O_3 than Fe_2O_3, the Cr_2O_3 will nucleate and grow preferentially at metal/solution interface, followed by the growth of Fe_2O_3. Finally, it causes the formation of the double layer structure of passive film [128-132].

Numerous works have been conducted to demonstrate that grain refinement benefits the corrosion resistance of passive film [133-136]. It was reported that passive film formed on nanocrystalline (NC) stainless steel is more compact and uniform than coarse crystalline (CC) stainless steels [135,137]. The reason can be attributable to the larger percentage of Cr^{3+} and Cr enriched in passive film or film/solution interface [138,139]. Additionally, it was also found that the passive film of sputtered NC stainless steel exhibits higher elastic modulus and hardness compared with conventional CC stainless steel [140].

3.1.3 Factors related with the breakdown of passive film

Grain boundaries as the preferentially dissolved sites, play a significant role in the breakdown of

passive films due to their nanostructural defects. These micro defects are characterized by nanopits with a dimension of several to dozens of nanometers and can be observed by STM or AFM images [141-144]. The formation of nanopits can be attributed to the competitive dissolution during the growth of oxide film preceding the stable passivity of the metal surface. Their sizes are increased by the increasing potential in passive region and chloride content. The nanopits with defective nature have less resistance to the migration of ions, thus, undergo less potential across oxide film at these sites. A larger potential drop applied at the metal/oxide interface will accelerate the dissolution of the oxide film at these sites, leading to passivity breakdown or the outwards diffusion of metal ions at the metal/solution interface. Finally, the collapse or ruptures in passive film appear [145,146].

The opinions concerning the role of Cl^- in the breakdown of passive films have great controversy. Evidences provided by some reports revealed that chloride was adsorbed on or incorporated into the passive film of stainless steel or Fe-Cr alloy, while other investigations presented the contradictory results [147-152]. Take a look at the experimental details, it will be found that the presence of Cl^- in the oxide film is associated with the growing condition of passive film. The passive film formed from a fresh surface in the Cl^- solution was observed to have the evidence of Cl^-, while passive film regrown from preformed passive film or air-formed oxide film in the Cl^- solution showed that Cl^- was not observed [153-156]. Therefore, it can be postulated that Cl^- can reduce the thickness of the oxide film by absorbing on the oxide film surface and disturbing film growth.

3.2 Hydrostatic pressure

Generally, field corrosion tests and laboratory experiments are adopted to investigate the corrosion of metallic materials in deep sea environment. The corrosion data obtained from field corrosion test is accurate and explicit while it is applicable for laboratory experiments to study the corrosion behavior in the mechanism aspects because of controllable factors.

3.2.1 Ocean depth in the field tests

Hydrostatic pressure is a unique factor for deep-sea ocean. It increases with water depth with 1atm increase for each increased 10m. The relation between this mysterious factor with corrosion arouses the interest of many research institutions. Investigations concerning field corrosion in deep-sea environment were initiated by the Civil Engineering–Naval Construction Battalion Center (NCEL), Port Hueneme, California in 1960. The testing specimens of 475 different alloys including cast iron, stainless steel, copper, nickel and aluminum were exposed in the Pacific Ocean at a depth of 762 and 1829m respectively. The effect of water depth on the general corrosion rate is not readily distinguished while aluminum and 6061-T6 alloy withstand a more severe pitting corrosion under deep-sea environment [157]. The information obtained from other researchers (Ulanovskii and Egorova [158,159], Reinhart [157], Melchers [160,161], Qin and Cui [162], Salau et al. [163], Sawant and Wagh [164], Venkatesan et al [165,166].) reveals that hydrostatic pressure has little influence on the weight loss of tested metals in a short-term corrosion duration and the reasons may be that oxygen concentration and water

temperature play a critical role in different immersion depths. Although the general corrosion of most metallic materials under varying immersion depths does not exhibit a significant difference, their local corrosion such as pitting corrosion and crevice corrosion specifically for passivated metals is affected by hydrostatic pressure indeed. Therefore, it is a need to conduct laboratory tests to evaluate the influence of hydrostatic pressure on the corrosion of metallic materials in depth.

3.2.2 Hydrostatic pressure in laboratory tests

According to Gutman's mechanistic chemistry theory [167], the change of potential, $\nabla\varphi$, on the metal surface, is related to the pressure exerted on its surface, which can be given by:

$$\nabla\varphi = -\frac{\Delta P V_m}{zF} \quad (5)$$

Where ΔP is external pressure, V_m is the molar volume of the matrix (m^3/mol), z is the valence of the element, and F is the Faraday constant. From equilibrium equation (5), it can be known that the increasing hydrostatic pressure reduces the potential of metal surface and promotes its dissolved activity.

It is demonstrated by many investigations that hydrostatic pressure is able to deteriorate the local corrosion of many metal materials from some aspects listed as Fig. 5. Beccaria et al. [168,169] found that hydrostatic pressure increases the pitting susceptibility of pure aluminum and 5086Al alloys. More localized corrosion zones and deeper pits was examined, suggesting that hydrostatic pressure increases the activity of Cl^-. Moreover, the increased permeability of Cl^- in passivation film changes the composition and structure of the passivation film, degrading its corrosion resistance. In their investigations, the passivated layer formed on pure aluminum is primarily composed of AlO(OH) at high pressure that has less corrosion resistance compared with the amorphous $Al(OH)_3$ layer formed at ambient pressure. Afterwards, the results offered by Junghans et al. indicate that the increasing hydrostatic pressure accelerates the interactions of the oxide film formed on the sputtered Al layer with Cl^- and H_2O in the preliminary stages of corrosion [170].

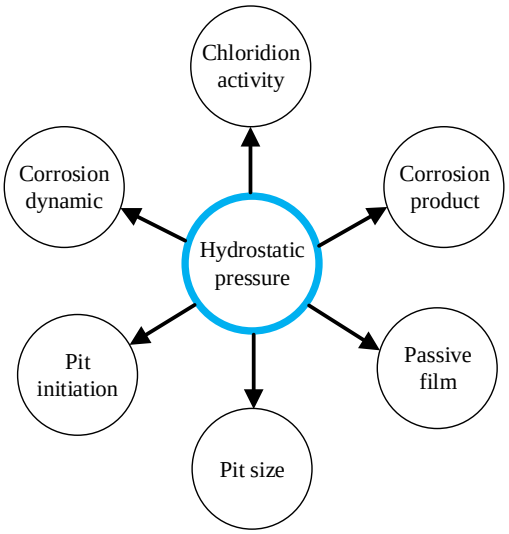

Figure 5. Possible influencing aspects of corrosion imparted by hydrostatic pressure.

Zhang et al [171]. investigated the effect of hydrostatic pressure on the pit corrosion of Fe-20Cr alloy using a stochastic analysis. Their results reveal that the pitting susceptibility of Fe-20Cr alloy is increased at high hydrostatic pressure, which is characterized by lower pitting potential and passive current accompanied by faster pit generation rate and larger metastable pits.

Zhang et al [172-179]. using high-resolution TEM and XPS to observe the difference of composition and structure in passive film of 316L stainless steel. Passive film obtained at 80 atm exhibits a more inhomogeneity in thickness compared to that at 1 atm, showing an evident thickness fluctuation. In addition, high hydrostatic pressure causes the decrease of the Fe(III)/Fe(II) ratio and Cr(III)-oxides in passive film, making it has lower stability. However, an investigation offered by Wang et al. indicates that pitting corrosion resistance is improved by increasing hydrostatic pressure, which are characterized by more noble pitting potential and larger charge transfer resistance [180].

Hydrostatic pressure also plays a significant role in the corrosion of low alloy steel. According to the reports from Yang et al. [181], hydrostatic pressure accelerates the anodic process and reduces the charge transfer resistance at the solid/liquid interface. Additionally, it promotes the initiation rate of metastable pitting and the growth probability of pits. However, the mechanism corresponding to these pitting phenomena of low alloy steel is not well distinguished so far. The corrosion pits of low alloy steel originate from inclusion of MnS both at high hydrostatic pressure and ambient pressure. But hydrostatic pressure accelerates pit growth parallel to the steel surface and the coalescence of neighboring pits [182]. Therefore, more severe uniform corrosion is observed [183]. For corrosion kinetics, it obviously accelerates the corrosion rate of low alloy steel in the initial immersion due to enhanced Cl^- adsorption and gives rise to the formation of more conductive rust layer [183-185].

3.3 Mechanical load

3.3.1 Elastic stress

In actual service condition, it is inevitable that metal structures withstand mechanical loads including stress and strain caused by equipment operation, which have a significant effect on the corrosion of metallic materials. Many studies have shown that stress (including constant and alternating stresses) can accelerate the corrosion rate of metallic materials [186-188].

The lattice defect density of the matrix surface is increased as applying external stress on its surface, which improves the nucleation probability of pits. Additionally, it is beneficial for stress to stimulate the interaction between precipitates and inclusions with their surrounding matrix, as a result, giving rise to the increase of dislocation density and atomic activation energy in the two-phase junction regions. That is, it enhances the dissolution of impurity phase. As the stress reaches a critical value, cracks will occur at the junction regions between matrix and inclusions, inducing the dissolution of matrix. Moreover, as the pits are formed, the stress will concentrate at the bottom of pitting cavity, leading to local deformation of corrosion pits, which enhances the corrosion attack on metallic materials [189-193].

Wang et al. [194] used the finite element method to study the effect of stress on the metastable pitting of stainless steel. It was found that stress significantly improves the pitting current of stainless

steels and decreases the incubation time of pits. It accelerates the evolution from metastable pitting to stable pitting. The effect of stress on the pitting potential of stainless steel is related with the number and size of the inclusions contained in steel. An investigation from Suter et al. [195] indicates that as the stainless steel exists a number of inclusions, the pitting potential shifts to more negative values meanwhile maintains a steady value as the inclusions are excluded.

The influence of stress on the corrosion behaviors of metals and alloys depends on its direction, size and distribution. Navai [196,197] 196 found that the passivation film formed on the surface of stainless steel under tensile stress condition has a greater thickness than compressive stress. Nevertheless, the passivation layer formed under compressive stress condition has higher Cr content and more dense structures than tensile stress. Decuzzi et al. [198] found that elastic stress has no effect on the corrosion potential of X100 steel. As the stress reaches a critical value, the atoms on the surface become unstable. It reacts with aqueous solution, causing the variation of surface morphology. Srolovitz [199] demonstrated the relationship between initial critical roughness wavelength, λ_c, and uniaxial elastic stress, σ^2, which is given by:

$$\lambda = \frac{\pi E \gamma}{(1-\nu^2)\sigma^2} \tag{6}$$

From Equation (6), it can be seen that for the surface with a smaller initial surface roughness, λ_c , a larger uniaxial elastic stress is needed to make the surface atoms unstable. It is necessary that the elastic stress reaches a certain critical value to accelerate the corrosion rate of metallic materials. Tang et al. [200] found that as the applied stress exceeds more than 80% of the yield strength of steel, the accelerated corrosion behavior on anodic dissolution becomes obvious. The initial surface roughness wavelength of steel depends on its phase compositions and grain sizes. Zhang et al.[201] found that the corrosion rate of sing-phase bainitic mild steel is greater than two-phase low alloy steel under elastic stress condition due to smaller initial surface roughness wavelength. The protective layers formed under dynamic loading condition have a higher charge transfer impedance than static loading condition. It indicates that steel suffers corrosion attack more easily under dynamic loading condition.

It is proposed by the related theory of surface stress / chemical reaction that chemical reaction proceeds along the direction of smoothing solid surface as no stress is applied due to the high dissolved activity of sharp peaks on metal surface, but making surface rougher under stress condition because the stress will concentrate on the bottom of scallops and stimulate the dissolution of matrix at these sites, as shown in Fig. 6 [202-206]. Therefore, precipitates generated by the hydrolysis and oxidation of the Fe^{2+}/Fe^{3+} in the solution preferentially grow along the direction of roughening substrate surface. The rust layers formed in this case have unsound structures with lower corrosion resistance. A report by Gao et al. shows that the rust layers formed under elastic load possess more porous structure, in which aggressive Cl^- can more easily diffuse from electrolyte to matrix surface. Therefore, the corrosion process is accelerated [207]. Yang et al. investigated the effect of stress distribution on the corrosion behavior of Q235 steel. They found that non-uniform stress distribution has an effect on the surface potential. It can cause the formation of galvanic couples on steel surface, stimulating the nucleation and pitting propagation of steel [208]. Ma et al. focused on the relationship between cyclic alternating load with the MnS-induced pitting corrosion behavior for A537 steel. It was found that the growth rate of pitting corrosion along the width direction is higher than the length and depth direction because of the

local plastic deformation along this direction. Meanwhile, cyclic stress amplitude had no evident effect on the pitting growth of pure aluminum. Nowadays, the influencing mechanism of cyclic alternating load on corrosion behavior of steel is not readily understood [209,210].

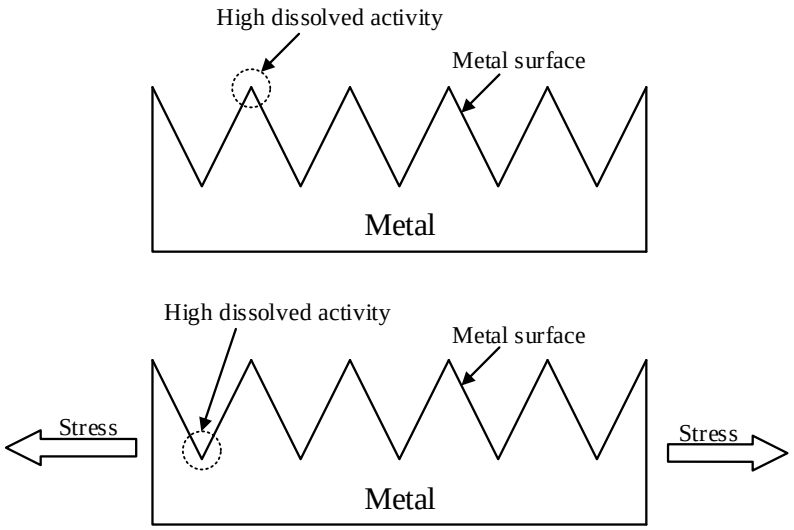

Figure 6. The effect of stress on surface roughness.

3.3.2 Plastic strain

As the stress is more than the yield strength, the material undergoes irreversible plastic deformation, and this part of deformation is denoted as plastic strain. Plastic deformation can lead to the generation and accumulation of dislocations. The dislocation density of steel increases with increasing deformation. The surface dislocation initiates to transfer into dislocation cells as the deformation increases to a threshold [211,212]. When the strain exceeds a critical value, martensitic transformation occurs on the steel surface [213-214]. In acidic solutions, the atoms near the dislocations have high activity, degrading the corrosion potential and accelerating the anodic dissolution of metal [215-217]. However, in special environments (such as the PEMFC environment), a certain amount of plastic deformation can enhance the corrosion resistance of steel because it inhibits the formation of hydroxide at dislocation sites, which is beneficial to the generation of protective oxides [211].

The comments concerned with the relationship between strain-induced martensitic transformation and the corrosion behavior of steel arouse a lot of controversy. A report from Mordyuk et al [214]. shows that strain-induced martensitic transformation not only improves the corrosion potential of 231 stainless steel, but also reduces the passivation current density. Meanwhile, Hamada et al. [218] did not observe the accelerated corrosion phenomenon caused by plastic-induced martensitic transformation.

Alvarez et al. found that the anodic dissolution rate of austenitic stainless steel is not only affected by the content of the transformed martensite, but also the distribution of martensite. The plastic deformation plays a more significant role in the acceleration of the corrosion process than elastic

deformation [219,220]. Gutman et al. [217] illustrated that a linear relationship between anodic dissolution rate with plastic deformation is not demonstrated. But interestingly, there is a peak that is related to the reorganization of dislocation groups.

Generally, dislocations and slip bands induced by strain are prone to roughen the steel surface. A plastic deformation-roughness variation model proposed by Dai and Chiang 190 is widely accepted, which is given by:

$$R = R_0 + kd\varepsilon \tag{7}$$

Where R is the surface roughness after plastic deformation, R_0 is the roughness before deformation, k is the coefficient, d is the grain size, and ε is the deformation. According to equation (8), it can be seen that the surface roughness related to the potential distribution presents a linear relationship with plastic strain [221,222].

The oxide film formed under plastic deformation conditions has more inhomogeneous structures and defects. It benefits the diffusion of aggressive anion across the oxide layer, deteriorating its corrosion resistance [223]. The uneven distribution of surface potential is prone to the formation of localized corrosion including crevice corrosion and pitting corrosion[224-225] . In addition, the junction regions between plastic deformation induced martensite and matrix is detrimental to the formation of passivated oxide layer and becomes the diffusion channels for aggressive ions [196]. Due to the significant difference in strength and toughness between the substrate and the formed oxide film, the oxide film is easy to rupture as the strain exceeds a critical value, ε_{crit}, which is given by:

$$\varepsilon_{crit} = \left(\frac{2\gamma}{A^2 f \pi E h}\right)^{0.5} \tag{8}$$

Where γ is the surface rupture energy (J/m^2), A is a coefficient, f is a constant between 0 to 1, and h is the thickness of the oxide film. Robert et al. found that strain with a low level do not affect the loss of rust formed on steel surface. As the strain applied is close to yield strain of the steel, significant mass loss and cracks appears [216].

4. CONCLUSION

Pitting corrosion as a localized accelerated dissolution of metal is initiated at the flaw or a breakdown site of passive film on the metal surface. The pitting process has been identified as distinct stages, namely pit initiation, metastable propagation and stable propagation. Some typical factors such as temperature, dissolved oxygen, salinity, pH, flaw rate have been reviewed by many researchers. In recent years, investigations about the influencing mechanism of oxide film, hydrostatic pressure and mechanical load on the corrosion of metallic materials have gathered much interest and attention.

Generally, passive film with several nanometers in thickness for stainless steels and Fe-Cr alloys has a bilayer structure composed of an Cr-oxide inner layer and Fe-oxide outer layer with an amorphous structure. 3D growth of passive film originates from a 2D adlayer, determining the structures and properties of passive film, which depends on the solution environment and potential. Grain boundaries play a significant role in the breakdown of passive films due to their nanostructure defects. Investigations from laboratory experiments reveal that hydrostatic pressure deteriorates the corrosion resistance of

many metallic materials including aluminum, aluminium alloys, Fe-Cr alloy, low alloy steel and nickel. Meanwhile it increases their pitting sensitivity. However, mechanism aspects about this field need further study. Mechanical load accelerates the corrosion of metallic materials via some mechanisms covering the generation of lattice defects density, accelerated interaction between inclusion and their surrounding matrix, concentration of stress in the corrosion pits, the change of potential distribution, and the breakdown of passive film. Distinguishing the single function of these factors and their inner connections is essential for understanding the corrosion mechanism of metals and alloys under multi-factor coupling conditions.

ACKNOWLEDGEMENTS
The authors would like to thank the financial supports from the National Natural Science Foundation of China (Project 51675533, 51701238 and 51705521).

References

1. S. Dexter, *Corrosion,* 36 (1980) 423.
2. M.G. Stewart, A. Al-Harthy, *Reliab. Eng. Syst. Saf.,* 93 (2008) 373.
3. L.T. Popoola, A.S. Grema, G.K. Latinwo, B. Gutti, A.S. Balogun, Int. J. Ind. Chem., 4 (2013) 1.
4. Y.M. Kolotyrkin, *Corrosion,* 19 (1963) 261.
5. Z. Szklarska-Smialowska, *Corrosion,* 27 (1971) 223.
6. Z. Szklarska-Smialowska, NACE International, Houston, 2005.
7. G.S. Frankel, *J. Electrochem. Soc.,* 145 (1998) 2186.
8. J. Soltis, *Corros. Sci.,* 90 (2015) 5
9. J. Bhandari, F. Khan, R. Abbassi, V. Garaniya, R. Ojeda, *J. Loss Prev. Process Ind.,* 37 (2015) 39.
10. R.M. Pidaparti, A.S. Rao, *Corros. Sci.,* 50 (2008) 1932.
11. K. Nisancioglu, H. Holtan, *Corros. Sci.,* 18 (1978) 835.
12. M. Pourbaix, L. Klimzack-Mathieu, C. Martens, J. Meunier, C. Vanlengenhaghe, L. Munch, J. Laureys, L. Nellmans, M. Warzee, *Corros. Sci.,* 3 (1963) 239.
13. N.J. Laycock, R.C. Newman, *Corros. Sci.,* 39 (1997) 1771.
14. N.J. Laycock, R.C. Newman, *Corros. Sci.,* 40 (1998) 887.
15. R.B. Inturi, Z. Szklarska-Smialowska, *Corros. Sci.,* 34 (1993) 705.
16. G.S. Frankel, R.C. Newman, C.V. Jahnes, M.A. Russak, *J. Electrochem. Soc.,* 140 (1993) 2192.
17. B.E. Wilde, E. Williams, *J. Electrochem. Soc.,* 118 (1971) 1057.
18. A.P. Bond, E.A. Lizlovs, *J. Electrochem. Soc.,* 115 (1968) 1130.
19. M. Janik-Czachor, *J. Electrochem. Soc.,* 128 (1981) 51.
20. M.N. Boucherit, D. Tebib, *Anti-Corros. Methods Mater.,* 52 (2005) 365.
21. Y.C. Tang, A.J. Davenport, *J. Electrochem. Soc.,* 154 (2007) C362.
22. L.Y. Xu, Y.F. Cheng, *Corros. Sci.,* 50 (2008) 2094.
23. B. Liu, T. Zhang, Y. Shao, G. Meng, J. Liu, F. Wang, *Int. J. Electrochem. Sci.,* 7 (2012) 1864.
24. K.D. Ralston, N. Birbilis, M.K. Cavanaugh, M. Weyland, B.C. Muddle, R.K.W. Marceau, *Electrochim. Acta,* 55 (2010) 7834.
25. Z.J. Zheng, Y. Gao, Y. Gui, M. Zhu, *Corros. Sci.,* 54 (2012) 60.
26. T. Shibata, M. Ameer, *Corros. Sci.,* 10 (1992) 1633.
27. H.J. Raetzer-Scheibe, *Corrosion,* 34 (1978) 437.
28. S.B. Basame, H.S. White, *J. Electrochem. Soc.,* 147 (2000) 1376.
29. T.P. Hoar, D.C. Mears, G.P. Rothwell, *Corros. Sci.,* 5 (1965) 279.
30. T.E. Pou, O.J. Murphy, V. Young, J. Bockris, L. Tongson, *J. Electrochem. Soc.,* 131 (1984) 1243.
31. C.Y. Chao, L.F. Lin, D.D. Macdonald, *J. Electrochem. Soc.,* 128 (1981) 1187.

32. T. Massoud, V. Maurice, L.H. Klein, P. Marcus, *J. Electrochem. Soc.,* 160 (2013) C232.
33. C.Y. Chao, L.F. Lin, D.D. Macdonald, *J. Electrochem. Soc.,* 129 (1982) 1874.
34. K. Sasaki, G.T. Burstein, *Corros. Sci.,* 38 (1996) 2111.
35. J.R. Galvele, *J. Electrochem. Soc.,* 123 (1976) 464.
36. N. Sato, *Electrochim. Acta,* 16 (1971) 1683.
37. T.P. Hoar, W.R. Jacob, *Nature,* 216 (1967) 1299.
38. H.H. Uhlig, *J. Electrochem.Soc.,* 97 (1950) 215C.
39. Y.M. Kolotyrkin, *J.Electrochem. Soc.,* 108 (1961) 209.
40. H.H. Uhlig, J.R. Gilman, *Corrosion,* 20 (1964) 289t.
41. K.E. Heusler, L. Fischer, *Werkst. Korros.,* 27 (1976) 551.
42. K.E. Heusler, L. Fischer, *Werkst. Korros.,* 27 (1976) 788.
43. Q. Song, R.C. Newman, R. Cottis, K. Sieradsky, *Corros. Sci.,* 31 (1990) 621.
44. D.E. Williams, R.C. Newman, Q. Song, R. Kelly, *Nature,* 350 (1991) 216.
45. G.T. Burstein, P.C. Pistorius, S.P. Mattin, *Corros. Sci.,* 35 (1993) 57.
46. A.M. Riley, D.B. Wells, D.E. Williams, *Corros. Sci.,* 32 (1991) 1307.
47. M.P. Ryan, N.J. Laycock, H.S. Isaacs, R.C. Newman, *J. Electrochem. Soc.,* 146 (1999) 91.
48. A. Pardo, M.C. Merino, A.E. Coy, F. Viejo, R. Arrabal, E. Matykina, *Corros. Sci.,* 50 (2008) 1796.
49. A.S. Mikhailov, J.R. Scully, J.L. Hudson, *Surf. Sci.,* 603 (2009) 1912.
50. C.M. Xu, Y.H. Zhang, G.X. Cheng, W.S. Zhu, Chin. *J. Chem. Eng.,* 14 (2006) 829.
51. A. Schneider, D. Kuron, S. Hofman, R. Kirchheim, *Corros. Sci.,* 31 (1990) 191.
52. T.Y. Jin, Y.F. Cheng, *Corros. Sci.,* 53 (2011) 850.
53. G.S. Eklund, *J. Electrochem. Soc.,* 121 (1974) 467.
54. J. Stewart, D.E. Williams, *Corros. Sci.,* 33 (1992) 457.
55. P. Schmuki, H. Hildebrand, A. Friedrich, S. Virtanen, *Corros. Sci.,* 47 (2005) 1239.
56. D.E. Williams, T.F. Mohiuddin, Y.Y. Zhu, *J. Electrochem. Soc.,* 145 (1998) 2664.
57. M.P. Ryan, D.E. Williams, R.J. Chater, B.M. Hutton, D.S. McPhail, *Nature,* 415 (2002) 770.
58. D.E. Williams, M.R. Kilburn, J. Cliff, G.I.N. Waterhouse, *Corros. Sci.,* 52 (2010) 3702.
59. T.Y. Jin, Y.F. Cheng, *Corros. Sci.,* 53 (2011) 850.
60. H. Wang, E. Han, *Electrochim. Acta,* 90 (2013) 128.
61. W. Tian, N. Du, S. Li, S. Chen, Q. Wu, *Corros. Sci.,* 85 (2014) 372.
62. K.S. Rao, K.P. Rao, *Trans. Indian Inst. Met.,* 57 (2004) 593.
63. G.T. Burstein, P.C. Pistorius, *Corros. Sci.,* 51 (1995) 380.
64. D.E. Williams, J. Stewart, P.H. Balkwill, *Corros. Sci.,* 36 (1994) 1213.
65. S.T. Pride, J.R. Scully, J.L. Hudson, *J. Electrochem. Soc.,* 141 (1994) 3028.
66. K.R. Zavadil, P.G. Kotula, J. Soltis, D. Krouse, *ECT Trans.,* 31 (2007) 207.
67. M.H. Moayed, R.C. Newman, *J. Electrochem. Soc.,* 153 (2006) B330.
68. J. Soltis, D. Krouse, S. Hodges, N. Laycock, K. Zavadil, S. Virtanen, P. Schmutz, M. Ryan, *ECS Trans.,* 25 (2010) 157.
69. Y.F. Cheng, M. Wilmott, J.L. Luo, *Appl. Surf. Sci.,* 152 (1999) 161.
70. G.T. Burstein, R.M. Souto, C. Liu, S.P. Vines, *Corros. Mater.,* 29 (2004) S1.
71. G.T. Burstein, C. Liu, R.M. Souto, S.P. Vines, *Corros. Eng. Sci. Technol.,* 39 (2004) 25.
72. P.C. Pistorius, G.T. Burstein, *Corros. Sci.,* 33 (1992) 1885.
73. P.C. Pistorius, G.T. Burstein, *Philos. Trans. R. Soc.,* 341 (1992) 531.
74. P.C. Pistorius, G.T. Burstein, *Corros. Sci.,* 36 (1994) 525.
75. G.S. Frankel, L. Stockert, F. Hunkeler, H. Böhni, *Corrosion,* 43 (1987) 429.
76. Y. Zhu, D.E. Williams, *J. Electrochem. Soc.,* 144 (1997) L43.
77. M.H. Moayed, R.C. Newman, *Corros. Sci.,* 48 (2006) 1004.
78. D.E. Williams, J. Stewart, P.H. Balkwill, *Corros. Sci.,* 36 (1994) 1213.
79. G.T. Burstein, R.M. Souto, *Electrochim. Acta,* 40 (1995) 1881.
80. H.B. Li, Z.H. Jiang, Y. Cao, Z.R. Zhang, *J. Metall. Mater.,* 16 (2009) 517.

81. G.T. Burstein, S.P. Mattin, *Philos.Mag. Lett.,* 66 (1992) 127.
82. V.M. Novakovski, A.N. Sorokina, *Corros. Sci.,* 6 (1966) 227.
83. H.I. Isaacs, G. Kissel, *J. Electrochem. Soc.,* 119 (1972) 1628.
84. H.I. Isaacs, *J. Electrochem. Soc.,* 120 (1973) 1456.
85. J.W. Tester, H.S. Isaacs, *J. Electrochem. Soc.,* 122 (1975) 1438.
86. S. Scheiner, C. Hellmich, *Corros. Sci.,* 49 (2007) 319.
87. T.P. Hoar, *Trans. Faraday Soc.,* 33 (1937) 1152.
88. J.R. Galvele, *J. Electrochem. Soc.,* 123 (1976) 464.
89. S. Hastuty, A. Nishikata, T. Tsuru, *Corros. Sci.,* 52 (2010) 2035.
90. S. Caines, F. Khan, J. Shirokoff, *J. Loss Prev. Process Ind.,* 26 (2013) 1466.
91. M.H. Moayed, N.J. Laycock, R.C. Newman, *Corros. Sci.,* 45 (2003) 1203.
92. J.R. Galvele, *Corros. Sci.,* 21 (1981) 551.
93. L. Oblonsky, T. Devine, *Corros. Sci.,* 37 (1995) 17.
94. H.H. Ge, G.D. Zhou, W.Q. Wu, *Appl. Surf. Sci.,* 211 (2003) 321.
95. C.O. Olsson, D. Landolt, *Electrochim. Acta,* 48 (2003) 1093.
96. X. Wang, D. Li, *Electrochim Acta,* 47 (2002) 3939.
97. H. Luo, C. Dong, K. Xiao, X. Li, *Appl. Surf. Sci.,* 258 (2011) 631.
98. T. Li, L. Liu, B. Zhang, Y. Li, X. Wang, F. Wang, *Electrochem. Commun.,* 52 (2015) 80.
99. M. Ryan, R. Newman, G. Thompson, *A Philos. Mag. B,* 70 (1994) 241.
100. J.A. Bardwell, G.I. Sproule, D.F. Mitchell, B. MacDougall, M.J. Graham, *J. Chem. Soc. Faraday Trans.,* 87 (1991) 1011.
101. J. Bardwell, G. Sproule, B. MacDougall, M. Graham, A. Davenport, H. Isaacs, *J. Electrochem. Soc.,* 139 (1992) 371.
102. W. Yang, D. Costa, P. Marcus, *J. Electrochem. Soc.,* 141 (1994) 2669.
103. E. Cho, H. Kwon, D.D. Macdonald, *Electrochim. Acta,* 47 (2002) 1661.
104. D. Hamm, K. Ogle, C.O. Olsson, S. Weber, D. Landolt, *Corros. Sci.,* 44 (2002) 1443.
105. R. Carranza, M. Alvarez, *Corros. Sci.,* 38 (1996) 909.
106. P. Marcus, J. Grimal, *Corros. Sci.,* 33 (1992) 805.
107. V. Maurice, W. Yang, P. Marcus, *J. Electrochem. Soc.,* 145 (1998) 909.
108. N. Hara, K. Sugimoto, *J. Electrochem. Soc.,* 138 (1991) 1594.
109. B. Zhang, J. Wang, B. Wu, X.W. Guo, Y.J. Wang, D. Chen, Y.C. Zhang, K. Du, E.E. Oguzie, X.L. Ma, *Nat. Commun.*, 9 (2018) 2559.
110. E. Hamada, K. Yamada, M. Nagoshi, N. Makiishi, K. Sato, T. Ishii, K. Fukuda, S. Ishikawa, T. Ujiro, *Corros. Sci.,* 52 (2010) 3851.
111. N.E. Hakiki, S. Boundin, B. Rondot, M.D.C. Belo, *Corros. Sci.,* 37 (1995) 1809.
112. N.E. Hakiki, M.D.C. Belo, A.M.P. Simoes, M.G.S. Ferreira, *J. Electrochem. Soc.,* 145 (1998) 3821.
113. Y. Gui, Z.J. Zheng, Y. Gao, *Thin Solid Films,* 599 (2016) 64.
114. J.Kunze, V. Maurice, L.H. Klein, H.-H. Strehblow, P. Marcus, *J. Phys. Chem. B,* 105 (2001) 4263.
115. J. Kunze, V. Maurice, L.H. Klein, H.-H. Strehblow, P. Marcus, *Electrochim. Acta,* 48 (2003) 1157.
116. J. Kunze, H.-H. Strehblow, G. Staikov, *Electrochem. Commun.,* 6 (2004) 132.
117. V. Maurice, H.H. Strehblow, P. Marcus, *Surf. Sci.,* 458 (2000) 185.
118. I. Betova, M. Bojinov, T. Laitinen, K. Mäkelä, P. Pohjanne, T. Saario, *Corros. Sci.,* 44 (2002) 2675.
119. X.Y. Wang, D.Y. Li, *Electrochim. Acta,* 47 (2002) 3939
120. W. Ye, Y. Li, F. Wang, *Electrochim. Acta,* 54 (2009) 1339.
121. G. Song, *Corros. Sci.,* 47 (2005) 1953.
122. A. Fattah-Alhosseini, A. Saatchi, M. Golozar, K. Raeissi, *Electrochim. Acta,* 54 (2009) 3645.
123. V. Maurice, W. Yang, P. Marcus, *J. Electrochem. Soc.,* 143 (1996) 1182.
124. B. Zhang, S. Hao, J. Wu, X. Li, C. Li, X. Di, Y. Huang. *Mater. Charact.,* 131 (2017) 168.

125. W.P. Yang, D. Costa, P. Marcus, *J. Electrochem. Soc.,* 141 (1994) 2669.
126. M.M. Hukovic, M.C. Ceric, *J. Electrochem. Soc.,* 134 (1987) 2193.
127. J.W. Schultze, M.M. Lohrengel, *Electrochim. Acta,* 45 (2000) 2499.
128. W. Ye, Y. Li, F.H. Wang, *Electrochim. Acta,* 51 (2006) 4426.
129. Z.J. Zheng, Y. Gao, Y. Gui, M. Zhu, *J. Solid State Electrochem.,* 18 (2014) 2201.
130. G. Lorang, M.D.C. Belo, A.P. Simoes, M.G.S. Ferreira, *J. Electrochem. Soc.,* 12 (1994) 3347.
131. K. Shimizu, H. Habazaki, P. Skeldon, G.E. Thompson, *Surf. Interface Anal.,* 35 (2003) 564.
132. Y. Gui, Z.J. Zheng, Y. Gao, *Thin Solid Films,* 599 (2016) 64.
133. S.G. Wang, M. Sun, K. Long, Z.D. Zhang, *Electrochim. Acta,* 112 (2013) 371.
134. P. Chen, L. Liu, Y. Li, B. Zhang, F.H. Wang, *J. Electrochem. Soc.,* 159 (2012) 453.
135. L. Liu, Y. Li, F.H. Wang, *Electrochim. Acta,* 52 (2007) 7193.
136. J. Lv, T. Liang, C. Wang, T. Guo, *J. Alloys Compd.,* 662 (2016) 143.
137. L. Liu, Y. Li, F.H. Wang, *Electrochim. Acta,* 53 (2008) 2453.
138. T.S. Li, L. Liu, B. Zhang, Y. Li, F.K. Yan, N.R. Tao, F.H. Wang, *Corros. Sci.,* 85 (2014) 331.
139. Z.J. Zheng, Y. Gao, Y. Gui, M. Zhu, *Corros. Sci.,* 54 (2012) 60.
140. T. Li, L. Liu, B. Zhang, Y. Li, X. Wang, F. Wang, *Electrochem. Commun.,* 52 (2015) 80.
141. D. Zuili, V. Maurice, P. Marcus, *J. Electrochem. Soc.,* 147 (2000) 1393.
142. J. Scherer, B.M. Ocko, O.M. Magnussen, *Electrochim. Acta,* 48 (2003) 1169.
143. A. Seyeux, V. Maurice, L.H. Klein, P. Marcus, *J. Solid State Electrochem.,* 9 (2005) 337.
144. F. Hahn, B. Beden, M.J. Croissant, C. Lamy, *Electrochim. Acta,* 24 (1986) 335.
145. P. Marcus, H.H. Strehblow, V. Maurice, *Corros. Sci.,* 50 (2008) 2698.
146. A. Seyeux, V. Maurice, P. Marcus, *Solid State Lett.,* 12 (2009) C25.
147. P.M. Natishan, W.E. O'Grady, F.J. Martin, R.J. Rayne, H. Kahn, A.H. Heuer, *ECS Trans.,* 41 (2012) 49.
148. A.R. Brooks, C.R. Clayton, K. Doss, Y.C. Lu, *J. Electrochem. Soc.,* 133 (1986) 2459.
149. S. Mischler, A. Vogel, H.J. Mathieu, D. Landolt, *Corros. Sci.,* 32 (1991) 925.
150. V. Mitrovic-Scepanovic, B. MacDougall, M.J. Graham, *Corros. Sci.,* 27 (1987) 239.
151. S. Ningshen, U.K. Mudali, V.K. Mittal, H.S. Khatak, *Corros. Sci.,* 49 (2007) 481.
152. C.O.A. Olsson, D. Landolt, *Electrochim. Acta,* 48 (2003) 1093.
153. C. Hubschmid, D. Landolt, *J. Electrochem. Soc.,* 140 (1993) 1898.
154. I. Olefjord, L. Wegrelius, *Corros. Sci.,* 31 (1990) 89.
155. W. Khalil, S. Haupt, H.H. Strehblow, *Mater. Corros.,* 36 (1985) 16.
156. A. Kocijan, C. Donik, M. Jenko, *Corros. Sci.,* 49 (2007) 2083.
157. F.M. Reinhart, Report Number TR-834, Civil Engineering Laboratory. Naval Construction Battalion Center, Port Hueneme, California, 1976, 265 pp.
158. I. Ulanovskii, *Prot. Met.,* 15 (1979) 563.
159. I. Ulanovskii, *V. Egorova, Prot. Met.,* 14 (1978) 137.
160. R.E. Melchers, *Corros. Sci.,* 50 (2008) 3446.
161. R.E. Melchers, *Corrosion,* 61 (2005) 895.
162. S. Qin, W. Cui, *Mar. Struct.,* 16 (2003) 15.
163. M. Salau, D. Esezobor, M. Omotoso, *Pet. Coal,* 53 (2011) 291.
164. S.S. Sawant, A.B. Wagh, *Corros. Prev. Control,* 37 (1990) 154.
165. R. Venkatesan, E.S. Dwarakadasab, M. Ravindrana, *Indian J. Eng. Mater. Sci.,* 10 (2003) 492.
166. R. Venkatesan, M.A. Venkatasamy, T.A. Bhaskaran, E.S. Dwarakadasa, M. Ravindran, *Br. Corros. J.,* 37 (2002) 257.
167. E.M. Gutman, Cambridge Interscience Publishing, Cambridge, 1998.
168. A.M. Beccaria, P. Ltraverso, G. Poggi, M.L. Lorenzetti, *High Pressure Res.,* 7 (1991) pp.347.
169. A.M. Beccaria, G. Poggi, *Br. Corros. J.,* 20 (1985) 183.
170. A. Junghans, R. Chellappa, P. Wang, J. Majewske, G. Luciano, R. Marcelli, E. Proietti, *Corros. Sci.,* 90 (2015) 101.

171. T. Zhang, Y. Yang, Y. Shao, G. Meng, F. Wang, *Electrochim. Acta,* 54 (2009) 3915.
172. C. Zhang, Z.W. Zhang, L. Liu, *Electrochim. Acta,* 210 (2016) 401.
173. C. Zhang, Z.W. Zhang, Q. Chen, L. Liu, *J. Alloys Compd.,* 758 (2018) 108.
174. L. Liu, C. Zhang, *Thin Solid Films,* 561 (2014) 70.
175. C. Yang, C. Zhang, W. Xing, L. Liu, *Intermetallics,* 94 (2018) 22.
176. Z. Li, C. Zhang, L. Liu, *J. Alloys Compd.,* 650 (2015) 127.
177. C. Zhang, H. Zhou, L. Liu, *Acta Mater.,* 72 (2014) 239.
178. P. Xu, C. Zhang, W. Wang, L. Liu, *Electrochim. Acta,* 206 (2016) 61.
179. M. Yasir, C. Zhang, W. Wang, P. Xu, L. Liu, *Mater. Des.,* 88 (2015) 207.
180. Z. Wang, Y. Cong, T. Zhang, *In. J. Electrochem. Sci.,* 9 (2014) 778.
181. Y. Yang, T. Zhang, Y. Shao, G. Meng, F. Wang, *Corros. Sci.,* 52 (2010) 2697.
182. Y. Yang, T. Zhang, Y. Shao, G. Meng, F. Wang, *Corros. Sci.,* 73 (2013) 250.
183. H. Sun, L. Liu, Y. Li, F. Wang, *J. Electrochem. Soc.,* 160 (2013) C89.
184. T. Kamimura, S. Hara, H. Miyuki, M. Yamashita, H. Uchida, *Corros. Sci.,* 48 (2006) 2799.
185. S. Hara, T. Kamimura, H. Miyuki, M. Yamashita, *Corros. Sci.,* 49 (2007) 1131.
186. E.M. Gutman, G. Solovioff, D. Eliezer, *Corros. Sci.,* 38 (1996) 1141.
187. J.Q. Wang, J. Li, Z.F. Wang, Z.Y. Zhu, W. Ke, Z.G. Wang, Q.S. Zang, *Scr. Metall. Mater.,* 11 (1993) 1415.
188. W. Staehle, *Corros. Sci.,* 49 (2007) 7.
189. J. Ma, B. Zhang, J.Q. Wang, G.Z. Wang, E.H. Han, W. Ke, *Corros. Sci.,* 52 (2010) 2867.
190. B. Chopard, L. Frachebourg, M. Droz, *Int. J. Mod. Phys. C,* 5 (1994) 47.
191. A. Turnbull, L. Wright, L. Crocker, *Corros. Sci.,* 52 (2010) 1492.
192. S. Ishihara, Z.Y. Nan, A.J. McEvily, T. Goshima, S. Sunada, *Int. J. Fatigue,* 30 (2008) 1659-1668.
193. R. Oltra, V. Vignal, *Corros. Sci.,* 49 (2007) 158.
194. H. Wang, E.H. Han, *Electrochim. Acta,* 90 (2013) 128.
195. T. Suter, E.G. Webb, H. Bohni, R.C. Alkirea, *J. Electrochem. Soc.,* 148 (2001) B174.
196. F. Nanai, *J. Mater. Sci.,* 30 (1995)1166.
197. E. Navai, O. Debbouz, *J. Mater. Sci.,* 34 (1999) 1073.
198. P. Decuzzi, G.P. Demelio, *Int. J. Solids Struct.,* 40 (2003) 729.
199. D.J. Srolovitz, *Acta Metall.,* 37 (1989) 621.
200. X. Tang, Y.F. Cheng, *Electrochim. Acta,* 54 (2009) 1499.
201. S. Zhang, X. Pang, Y. Yang, K. Gao, *Corros. Sci.,* 75 (2013) 293.
202. H.H. Yu, *J. Solids Struct.,* 42 (2005) 3852.
203. L.B. Freund, *Int. J. Solids Struct.,* 32 (1995) 911.
204. J.H. Prevost, T.J. Baker, J. Liang, Z. Suo, *Int. J. Solids Struct.,* 38 (2001) 5185.
205. W. Mullins, *J. Appl. Phys.,* 30 (1959) 77.
206. H.H. Yu, Z. Suo, *J. Appl. Phys.,* 87 (2000) 1211.
207. K. Gao, D. Li, X. Pang, S. Yang, *Corros. Sci.,* 52 (2010) 3428.
208. H.Q. Yang, Q. Zhang, S.S. Tu, Y. Wang, Y.M. Li, Y. Huang, *Corros. Sci.,* 110 (2016) 1.
209. J. Ma, B. Zhang, J. Wang, G. Wang, E.H. Han, W. Ke, *Corros. Sci.,* 52 (2010) 2867.
210. S. Ishihara, Z.Y. Nan, A.J. McEvily, T. Goshima, S. Sunada, *Int. J. Fatigue,* 30 (2008) 1659.
211. J. Lu, T. Liang, W. Guo, *Int. J. Hydrogen Energy,* 40 (2015) 10382.
212. Z. Cui, Z. Liu, L. Wang, X. Li, C. Du, X. Wang, *Mater. Sci. Eng. A,* 677 (2016) 259.
213. F.K. Yan, G.Z. Liu, N.R. Tao, K. Lu, *Acta Mater.,* 60 (2012) 1059.
214. B.N. Mordyuk, G.I. Prokopenkoa, M.A. Vasylyev, M.O. Iefimov, *Mater. Sci. Eng. A,* 458 (2007) 253.
215. A.I. Rusanov, N.B. Uriew, P.V. Eryukin, T.G. Movchan, N.E. Esipova, *Mendeleev Commun.,* 14 (2004) 58.
216. R.E. Melchers, J.Kee. Paik, *Corros. Sci.,* 51 (2009) 2298.
217. E.M. Gutman, G. Solovioff, D. Eliezer, *Corros. Sci.,* 38 (1996) 1141.

218. A.S. Hamada, L.P. Karjalainen, M.C. Somani, *Mater. Sci. Eng. A,* 431 (2006) 211.
219. S.M. Alvarez, A. Bautista, F. Velasco, *Corros. Sci.,* 69 (2013) 130.
220. A. Nazarov, V. Vivier, D. Thierry, F. Vucko, B. Tribollet, *J. Electrochem. Soc.,* 164 (2017) C66.
221. W. Li, D.Y. Li, *Acta Mater.,* 54 (2006) 445.
222. H. Krawiec, V. Vignal, E. Schwarzenboeck, J. Banas, *Electrochim. Acta,* 104 (2013) 400.
223. A. Barbucci, G. Cerisola, P.L. Cabot, *J. Electrochem. Soc.,* 149 (2002) B534.
224. V. Vignal. C. Valot, R. Oltra, M. Verneau, L. Coudreuse, *Corros. Sci.,* 44 (2002) 1477.
225. P.M.O. Silva, H.F.G. Abreu, V.H.C. Albuquerque, P.L. Neto, J.M.R.S. Tavares, *Mater. Des.,* 32 (2011) 605.